Electric driving of magnetization dynamics in a hybrid insulator

Cong Xiao,* Bangguo Xiong,* and Qian Niu
Department of Physics, The University of Texas at Austin, Austin, Texas 78712, USA

(Received 19 January 2021; revised 17 June 2021; accepted 4 August 2021; published 19 August 2021)

Established forms of electromagnetic coupling are usually conservative (in insulators) or dissipative (in metals and semiconductors). Here, we point out the possibility of nondissipative electric driving of magnetization dynamics, if the valence electronic states have nontrivial topology in the combined space of crystal momentum and magnetization configuration. We provide a hybrid insulator system to demonstrate that the topology-based nonconservative electrical generalized force is capable of supporting sustained magnetization motion in the presence of Gilbert damping, with quantized and steady energy pumping into magnetization motion from the electric field. We also generalize our results to magnetic textures, and discuss an electric-field-induced Dzyaloshinskii-Moriya interaction which can be nonconservative.

DOI: 10.1103/PhysRevB.104.064433

I. INTRODUCTION

The study of the electrical control of magnetization dynamics has occupied a large part of solid state research for many decades, which generally falls into two separate categories known as multiferroics [1–3] and spintronics [4] depending on the conductive behavior of the hosting materials. The former deals with insulators where the electrical effects on magnetization are characterized through the free energy [5], and the resulting torque would be naturally considered as conservative and unable to drive the sustained motion of the magnetization for a static electric field. In the latter, one finds various current-induced magnetic torques in metals and semiconductors [6–8], which can provide a persistent source of energy for the sustained motion of magnetization, but one has to deal with wasteful and prohibitive Joule heating in practice.

Magnetic insulators have recently been utilized to achieve low-dissipation magnetization control by combining the insulator with heavy metals hosting a prominent spin Hall effect that injects a spin current into the insulator [9,10]. An electric field can also directly manipulate magnetization in an insulator without Joule heating by means of spin-orbit torques mediated by occupied electronic states [11–13]. In particular, mesoscopic transport theories proposed the exchange gapped edge states of a two-dimensional topological insulator combined with a magnet as a unique platform for studying the magnetic Thouless motor [14,15], which works as the inverse mode of the adiabatic charge pumping by a cyclic magnetic motion [16–18] under an applied voltage. By using the scattering matrix approach [19], previous works showed quantized electrical energy transfer into the magnet if the magnetization accomplishes a cyclic motion [14,15]. On the other hand, as the Berry curvature in the mixed space of crystal momentum and magnetization configuration underlies magnetic Thouless pumping, it would be interesting to reveal the relation between nonzero electrical energy input into magnetic dynamics and the topological characteristics in the mixed parameter space [20]. Moreover, it has not been shown whether the electric driving of sustained magnetic motion, which enables a motor, can be realized in the presence of magnetic damping due to the coupling of magnetization to degrees of freedom other than electrons.

In this paper we show the possibility of nondissipative driving of magnetization dynamics with steady energy pumping by a static electric field in insulators. This is motivated by the fact that electric polarization is not always a single-valued quantity [21,22], and the adiabatic current pumped by the cyclic motion of the magnetization can acquire a quantized net amount of energy from a static electric field under certain topological conditions of the valence electronic states. We exploit this idea in a model system of edge states of a two-dimensional topological insulator gapped by a hybrid with a magnetic wire, and show explicitly sustained magnetization motion when a constant electric field is applied to overcome Gilbert damping.

Our results can also be generalized to the case of slowly varying magnetic textures. There is a topological current bilinear in the gradient and time derivative of the magnetization density [23], a sort of anomalous Hall current induced by the artificial electric field from a time-dependent magnetic texture [24–27]. This current provides a channel of nondissipative drive of the magnetic texture by an external static electric field. In topologically nontrivial cases this drive is nonconservative and capable of delivering a nonzero and quantized amount of energy when the magnetic texture wraps around the Bloch sphere in time. In topologically trivial cases, where the electric polarization induced by a magnetization gradient is well defined, the drive is conservative because it can be identified as originating from a polarization energy density whose susceptibility to the magnetization gradient gives the electric-field-induced Dzyaloshinskii-Moriya interaction (DMI) [28–31].

*These authors contributed equally to this work.

 ©2021 American Physical Society

The rest of the paper is organized as follows. In Sec. II we focus on the electric-field-induced generalized force on a homogeneous magnetization in insulators, and study its nonconservative nature which is related to certain topological conditions of the occupied electronic states. These general rationales are illustrated in a hybrid insulator in Sec. III, in which the electric driving of sustained magnetic motion is also demonstrated. Section IV is devoted to the electrical generalized force on the magnetization in inhomogeneous insulators and its relation to an electric-field-induced DMI. Finally, we conclude the paper in Sec. V.

II. ELECTRICAL GENERALIZED FORCE ON MAGNETIZATION

In the language of analytic mechanics, a generalized force is an amount of work done on the system per unit displacement in the dynamical variable (the magnetization here). Considering a system with a homogeneous magnetization $\boldsymbol{m}$ coupled to an electronic insulator, the change in the magnetization can in general pump an adiabatic electric current

$$\boldsymbol{j} = e \int [d\boldsymbol{k}] \Omega_{\boldsymbol{km}} \cdot \dot{\boldsymbol{m}}, \tag{1}$$

where $\Omega_{\boldsymbol{km}}$ is the electronic Bloch-state Berry curvature in the parameter space of the magnetization and crystal momentum $\boldsymbol{k}$ (set $\hbar = 1$ unless otherwise noted), with its Cartesian components given by $-2\,\mathrm{Im}\langle\partial_{k_i} u|\partial_{m_j} u\rangle$. Here, $|u\rangle$ is the periodic part of the Bloch wave, and the band index n is omitted for simple notation. $[d\boldsymbol{k}] \equiv d^d k/(2\pi)^d$ with d as the spatial dimension, and the summation over valence bands is implied. Through this adiabatic current, an external electric field can deliver work on the system, with the work density $\delta w = \boldsymbol{E} \cdot \boldsymbol{j} dt$, which is proportional to $\delta \boldsymbol{m} = \dot{\boldsymbol{m}} \cdot dt$. Therefore, we obtain the electrical generalized force density on magnetization as

$$\boldsymbol{E}^e_m \equiv \frac{\delta w}{\delta \boldsymbol{m}} = e\boldsymbol{E} \cdot \int [d\boldsymbol{k}] \Omega_{\boldsymbol{km}}. \tag{2}$$

This electrical generalized force is nondissipative because of the lack of conduction electrons for Joule heating, and is in fact topological in the sense that it delivers a quantized amount of energy over a cycle of the magnetization motion. For simplicity, we first consider an insulator with zero Chern numbers in the Brillouin zone at each point over the path of $\boldsymbol{m}$, such that one can take a $\boldsymbol{k}$-space periodic gauge to locally define an electronic polarization $\boldsymbol{P} = -e \int [d\boldsymbol{k}] \boldsymbol{\mathcal{A}}_{\boldsymbol{k}}$ [21], with $\boldsymbol{\mathcal{A}}_{\boldsymbol{k}} = \langle u|i\partial_{\boldsymbol{k}} u\rangle$. Then the electrical work density delivered over the cycle can be written in terms of the change of this polarization,

$$w = \oint d\boldsymbol{m} \cdot \boldsymbol{E}^e_m = \boldsymbol{E} \cdot \Delta \boldsymbol{P}. \tag{3}$$

This change is quantized in units of $\Delta \boldsymbol{P} = -e\boldsymbol{a}/V_0$ with $\boldsymbol{a}$ being a discrete lattice vector (including the null vector) and V_0 the volume of a unit cell. When this change is zero, so that the polarization is globally defined, the electrical generalized force is conservative in the sense that its work can be regarded as a change in the globally well-defined polarization energy density $-\boldsymbol{E} \cdot \boldsymbol{P}$. When this change is nonzero, the electrical generalized force is nonconservative and capable of supporting sustained magnetization motion even in the presence of Gilbert damping due to other dissipative channels.

Some comments are in order. First, if the electronic insulator is one dimensional, then the electrical work (per unit length) over a cycle of the magnetization reduces to eE times the Chern number over the torus of the combined space of crystal momentum and the magnetization (along its path), corresponding to the quantized number of electrons pumped over the cycle. Second, quantization of electrical work over the cycle of magnetization also applies to insulators with nonzero $\boldsymbol{k}$-space Chern numbers by a simple argument. Although one cannot take a periodic gauge in $\boldsymbol{k}$ space, one can always choose a periodic gauge over a fixed one-dimensional path of the magnetization. It is then clear that the electrical work over the cycle equals the Brillouin-zone integral of the $\boldsymbol{k}$ gradient of the Berry's phase over the cycle. Topological quantization of this work then follows from the multivaluedness of the Berry's phase. Third, using the Bianchi identity on Berry curvatures, one can easily show that the electrical generalized force is curl-free $\partial_{\boldsymbol{m}} \times \boldsymbol{E}^e_m = 0$ everywhere in $\boldsymbol{m}$ space, except the singular points where the energy gap above the filled states of the electron system closes.

When can the electrical work on magnetization be nonzero? The quantization of its value implies that the electrical work is invariant if the path in $\boldsymbol{m}$ space is deformed without closing the energy gap. In particular, within a singly connected region where the gap is open, the electrical work is zero on all closed paths. This applies for example to the north or south hemispheres of magnetization in the two-dimensional ferromagnetic Dirac model studied in Ref. [32], where one can define polarization energies separately for each region, although not globally because of the gap closing on the equator. Consequently, this model system cannot provide nonzero electrical work for sustained magnetization motion. It is therefore clear that the singular points of gap closing have to be arranged to define multiply connected regular regions, where electrical work can possibly be nonzero on topologically nontrivial paths.

III. A MODEL FOR SUSTAINED MAGNETIZATION MOTION

Here, we propose a one-dimensional model system, where the gap closes on the two poles of the magnetization Bloch sphere, and the electrical work per unit length is eE times the winding number of the path around the poles. The system is constructed by interfacing a magnetic wire with the topological edge states of a two-dimensional topological insulator (Fig. 1). The exchange coupling renders the electronic system insulating by opening a gap in the Dirac spectrum. The relevant low-energy Hamiltonian is

$$\hat{h} = \hbar v k \hat{\sigma}_y + J\hat{\boldsymbol{\sigma}} \cdot \boldsymbol{m}, \tag{4}$$

where v is the Fermi velocity, $\hat{\boldsymbol{\sigma}}$ is the Pauli matrix, and J is the coupling constant. The magnetization $\boldsymbol{m}$ is assumed to have a fixed magnitude and is parametrized by the polar angle θ relative to the y axis and the azimuthal angle ϕ as shown in Fig. 1. The energy gap is open everywhere except at the north and south poles of the Bloch sphere with $m_y = \pm m$ (red dots).

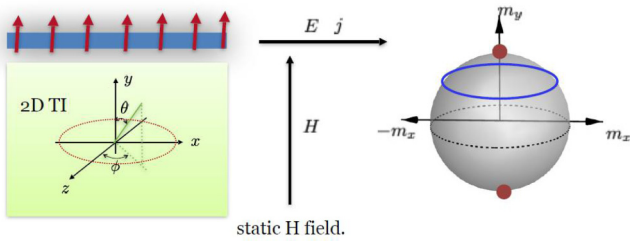

FIG. 1. A ferromagnetic wire (blue bar) hybridizes and gaps the edge states of a two-dimensional topological insulator (green region). When the magnetization $\boldsymbol{m}$ moves around (blue circle on the right) on the Bloch sphere, the pumped adiabatic current j along the edge couples to an applied electric field $\boldsymbol{E}$ to provide energy to overcome Gilbert damping. A static magnetic field $\boldsymbol{H}$ is applied to help prepare the system into a sustained motion of limit cycle.

Assuming that the lower band is filled and the electric field is applied along the magnetic wire (positive x direction), we can evaluate the formula for the electrical generalized force to find

$$\boldsymbol{E}^e = \frac{-eE}{2\pi m}\frac{\hat{\boldsymbol{e}}_\phi}{\sin\theta} = -eE\frac{\partial_{\boldsymbol{m}}\phi}{2\pi}. \tag{5}$$

It is singular at the poles and is a gradient of the multiple-valued azimuthal angle, so that the electrical work density over a closed path on the Bloch sphere is quantized in terms of the winding number of the path,

$$\oint d\boldsymbol{m}\cdot\boldsymbol{E}^e = -N_t eE, \tag{6}$$

in line with the aforementioned general topological arguments. The winding number N_t counts how many times the closed path wraps around the y axis counterclockwise.

In such a one-dimensional insulator it is also interesting to understand the electrical generalized force from the polarization as $\boldsymbol{E}^e = E\partial_{\boldsymbol{m}}P$, where the polarization is not single valued and can only be determined to be $P = -e\phi/2\pi$ up to an uncertainty quantum $-e$. Consistently, the two gap closing poles are singular points of the polarization, and the change of polarization upon a closed path on the Bloch sphere is $-eN_t$.

We now proceed to study the dynamics of the magnetization to see the effect of this generalized force. In the absence of coupling to the electronic system, we can rewrite the Landau-Lifshitz-Gilbert equation of the ferromagnet in the form of $-\partial_{\boldsymbol{m}}\mathcal{G}^0 + \dot{\boldsymbol{m}}\times\boldsymbol{\Omega}^0_{\boldsymbol{m}} - \eta^0\dot{\boldsymbol{m}} = 0$, as balancing out a conserved force from the free energy $\mathcal{G}^0$, a Lorentz-type force from the $\boldsymbol{m}$-space Berry curvature $\boldsymbol{\Omega}^0_{\boldsymbol{m}}$ [33], and a frictional force with a scalar damping coefficient η^0. We will model the free-energy density as $\mathcal{G}^0 = -K^0\hat{m}_x^2 - Hm_y$ with an easy-axis anisotropy and an applied static magnetic field H. The $\boldsymbol{m}$-space Berry curvature is given in terms of the gyromagnetic ratio γ^0 as $\boldsymbol{\Omega}^0_{\boldsymbol{m}} = \boldsymbol{m}/(m^2\hbar\gamma^0)$. The damping coefficient is related to the Gilbert number λ as $\lambda = (\gamma^0)^2\eta^0$.

In the presence of coupling to the electronic system, the equation of motion becomes

$$\boldsymbol{E}^e_m - \partial_{\boldsymbol{m}}\mathcal{G} + \dot{\boldsymbol{m}}\times\boldsymbol{\Omega}_{\boldsymbol{m}} - \eta\dot{\boldsymbol{m}} = 0, \tag{7}$$

where the electrical generalized force enters as an extra term along with electronic modifications to the other terms. The gap opening in the electronic system contributes a lowering of

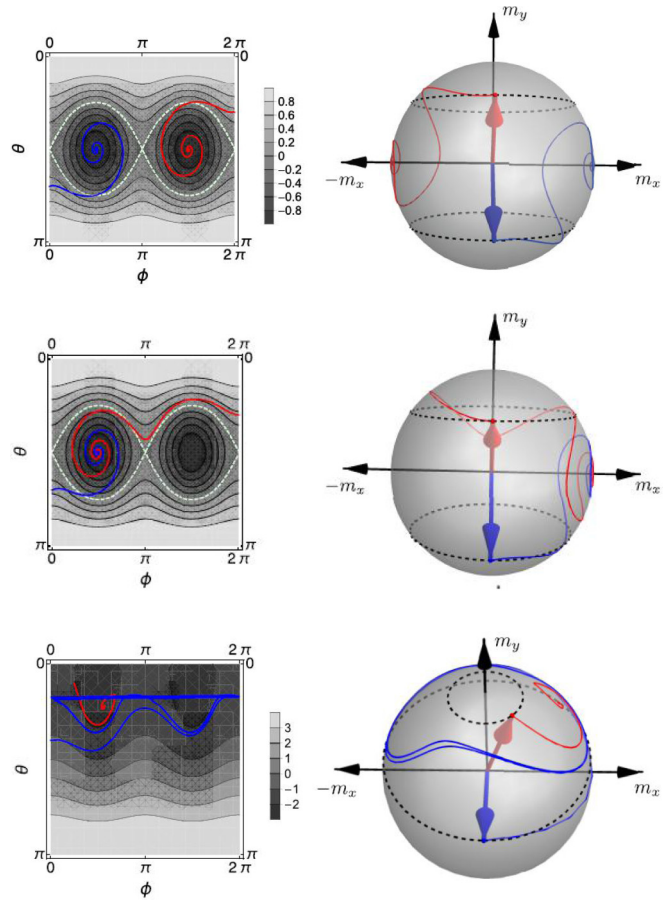

FIG. 2. Free-energy contours in the angular space and typical evolution trajectories on the Bloch sphere in the absence (top panels) and presence (middle panels) of an electric field, and in the presence of both electric and magnetic fields (bottom panels). In the last case, a limit cycle emerges.

the free energy $\mathcal{G}^e = K^e(\hat{m}_y^2 - 1)$ that we model as a hard-axis anisotropy. The electronic contribution to the $\boldsymbol{m}$-space Berry curvature is given by $\boldsymbol{\Omega}^e_{\boldsymbol{m}} = \int[d\boldsymbol{k}]\Omega_{\boldsymbol{m}} = \boldsymbol{m}/(m^2\hbar\gamma^e)$, where $\Omega_{\boldsymbol{m}} = \partial_{\boldsymbol{m}}\times\boldsymbol{\mathcal{A}}_{\boldsymbol{m}}$ is derived from $\boldsymbol{\mathcal{A}}_{\boldsymbol{m}} = \langle u|i\partial_{\boldsymbol{m}}u\rangle$, and $\gamma^e = 2\pi v/J$. Finally, we assume that the gap of the electronic system remains open during the course of dynamics, so there is no electronic contribution to the damping coefficient $\eta = \eta^0$.

Representative results of the magnetization motion are presented in Fig. 2, where we take $\gamma^e/\gamma^0 = \pi$, $K^e/(m/\gamma^0) = K^0/(m/\gamma^0) = 1$ GHz, and $\eta = 0.2/(m\gamma^0)$. Shown in the top and middle panels ($H = 0$), there are two types of energy conserved motion in the absence of damping and external fields, divided by the contour of zero energy (the white dashed curve). In the area enclosing the two points of lowest energy, $\boldsymbol{m}$ rotates around the x axis, whereas in the upper and lower areas outside of the zero-energy contour $\boldsymbol{m}$ goes around the y axis. This situation is changed in the presence of damping, as shown in the top panel, where two points $(\phi = 0, \theta = 0.3\pi)$ and $(\phi = 0, \theta = 0.7\pi)$ outside of the zero-energy contour evolve to different points of lowest energy. In the middle panels, an electric field $eE/2\pi = 0.1K^0$ is applied, which gives a force in the clockwise (negative ϕ) direction. The blue

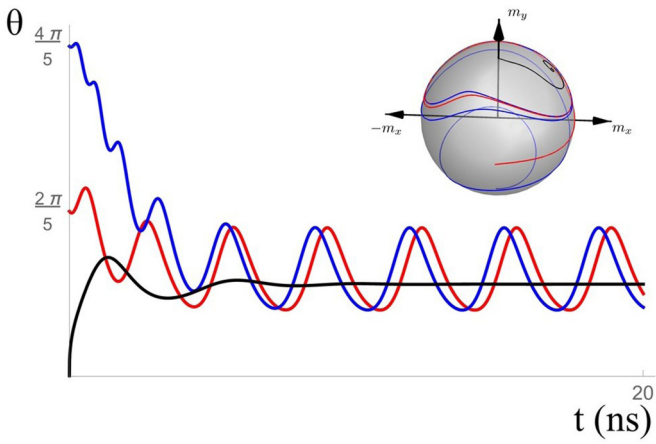

FIG. 3. Time dependence of the polar angle for different initial conditions, $\phi = 0$, $\theta = 0.001\pi$ (black), $\theta = 0.4\pi$ (red), $\theta = 0.8\pi$ (blue). Correspondingly on the Bloch sphere shown in the inset, the red and blue trajectories evolve into a right-handed limit cycle, whereas the black trajectory evolves into the point of lowest energy.

trajectory starting from $(\phi = 0, \theta = 0.7\pi)$ falls faster to the $+m_x$ axis, while the red trajectory starting from $(\phi = 0, \theta = 0.3\pi)$ extends for 3/4 circle before the final decay into the same energy minimum as the other trajectory.

The lower panels show the situation where the limit cycle motion is found. We found it important to prepare the system with predominantly around-m_y-axis energy contours, so that the nonconservative electrical force can be best utilized. We therefore apply a static magnetic field in the y direction with the magnitude $H = K^0/m$ to change the energy landscape. We also switched the direction of the electric field so that the electrical force goes along the directions of the energy contours. We found that all initial points in a wide region, between the two dashed circles shown on the right of the lower panels of Fig. 2, fall into the same limit cycle. For instance, the blue curve starts from $(\phi = 0, \theta = 0.4\pi)$ and evolves into the right-handed limit cycle under an electric field $eE/2\pi = -0.1K^0$. Figure 3 shows how the limit cycle motion is reached in time for two trajectories (blue and red) from different initial angles, along with one (black) that falls into an energy minimum. On the limit cycle, we found that the energy input from the electrical force balances out the energy dissipation from the Gilbert damping, $\oint d\boldsymbol{m} \cdot (\boldsymbol{E}^e_m - \eta \dot{\boldsymbol{m}}) = 0$, as can be easily derived from the equation of motion.

IV. ELECTRICAL DMI FORCE

So far we have been concentrating on nondissipative electrical driving on a uniform magnetization. When the magnetization is nonuniform, the electrical generalized force Eq. (2) still applies as a local force density, but there will be additional contributions due to the magnetization gradients. In metals, the electric-current-induced DMI has been discussed recently [34–36], which is similar to the current-induced orbital magnetization [37,38]. The intrinsic analog, the electric-field-induced nondissipative DMI [1,39], remains elusive in the band picture, but should be well defined in insulators as we show now.

To first order in the gradient, there is an adiabatic current pumped by the magnetization dynamics [23] $\boldsymbol{j} = e\int [d\boldsymbol{k}]\Omega_{\boldsymbol{k}[\boldsymbol{k}\boldsymbol{r}]\boldsymbol{m}} \cdot \dot{\boldsymbol{m}}$ involving the second Chern form of Berry curvatures $\Omega_{k_s[\boldsymbol{k}\boldsymbol{r}]m_j} \equiv \Omega_{k_s k_i}\Omega_{r_i m_j} + \Omega_{k_s r_i}\Omega_{m_j k_i} + \Omega_{k_s m_j}\Omega_{k_i r_i}$. Through this current, an external electric field can produce a work density $\delta w = \boldsymbol{E} \cdot \boldsymbol{j} dt$ proportional of δm, implying an electrical generalized force linear in the magnetization gradient,

$$\boldsymbol{E}^e_m = e\boldsymbol{E} \cdot \int [d\boldsymbol{k}]\Omega_{\boldsymbol{k}[\boldsymbol{k}\boldsymbol{r}]\boldsymbol{m}}. \tag{8}$$

For reasons to be discussed later, we will call this an electrical DMI force, although it is nonconservative in general and capable of sustained driving of magnetization textures.

Because the second Chern form is antisymmetric in the crystal momentum, a nonzero result demands that the electronic system is more than one dimensional. Consider for simplicity a two-dimensional system with the magnetization gradient in the y direction (one-dimensional domain wall or a spiral) and an electric field applied in the transverse x direction. The electrical work per unit transverse width over one pumping period may be written as

$$W = eE_x N_{yt} \int_{T^2} \frac{d^2k}{2\pi} \int_{S^2} \frac{d\theta d\phi}{2\pi} \Omega_{k_x k_y \theta\phi} = eE_x N_{yt} C_2, \tag{9}$$

which is topological and quantized in terms of the second Chern number C_2 in the space [40] spanned by the Brillouin zone and the Bloch sphere, and the winding number $N_{yt} = \frac{1}{4\pi}\int dydt\hat{\boldsymbol{m}} \cdot (\partial_y \hat{\boldsymbol{m}} \times \partial_t \hat{\boldsymbol{m}})$ for the mapping $\hat{\boldsymbol{m}}(y,t)$ of the yt space-time onto the Bloch sphere [41] ($\hat{\boldsymbol{m}} = \boldsymbol{m}/m$). This winding number previously appeared in a discussion of quantized electromotive force induced by a moving domain wall [42], the so-called ferro-Josephson effect, and the second Chern number may be regarded as the quantum measure of the anomalous Hall response to this emf [43]. The quantized electrical work is therefore a result of this quantized Hall current in the direction of the applied electric field.

The same second Chern number has also been introduced in the study of electric charges carried by magnetic textures such as a skyrmion [30], where it may be understood as the quantum measure of charge response to the quantized flux of an artificial magnetic field [43]. This is a sort of Streda dual effect of the quantum Hall current response to the artificial electric field of the magnetic texture. This relationship becomes especially clear in the absence of spin-orbit coupling, where $\Omega_{k_x k_y \theta\phi} = \Omega_{k_x k_y}\Omega_{\theta\phi}$ and C_2 reduces to the first Chern number in $\boldsymbol{k}$ space [44] which characterizes the usual quantum anomalous Hall insulators.

In non-Chern insulators where one may choose a periodic gauge in $\boldsymbol{k}$ space, the electrical generalized force may be written as a field derivative of the polarization energy, $\boldsymbol{E}^e_m = -\delta_{\boldsymbol{m}} U$, with [30,31]

$$U = -\int d\boldsymbol{r}\boldsymbol{E} \cdot \boldsymbol{P} = \int d\boldsymbol{r}\mathcal{D}_{il}\partial_i m_l, \tag{10}$$

where $\boldsymbol{P}$ is the electric polarization induced by a magnetization gradient, including a topological Chern-Simons part [23] for which

$$\mathcal{D}_{il} = \frac{e}{2}E_j \int [d\boldsymbol{k}]\left(\mathcal{A}_{k_j}\Omega_{k_i m_l} + \mathcal{A}_{k_i}\Omega_{m_l k_j} + \mathcal{A}_{m_l}\Omega_{k_j k_i}\right). \tag{11}$$

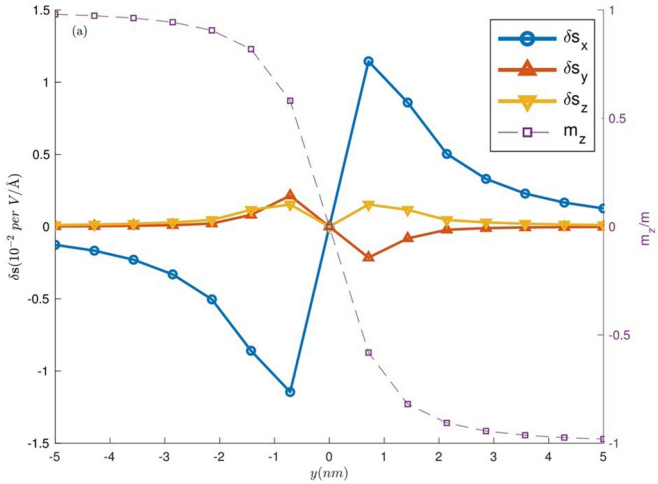

FIG. 4. Spin generation due to the electrical generalized force in a model of chiral Néel wall of ferromagnetic transition metal dichalcogenide monolayer.

However, this expression for the DMI coefficient is only locally defined because of the gauge dependence of the Chern-Simons form [45].

On the other hand, the electrical DMI force $\boldsymbol{E}_m^e$ [Eq. (8)] is not only gauge invariant and single valued but also well defined for Chern insulators. In practice, such a force enters directly in determining the static and dynamic behavior of the magnetic textures. For example, we show in the following that the width of a chiral Néel wall may be tuned by such a force, as would normally be anticipated from DMI effects [34,35]. Specifically, we consider a chiral Néel wall with easy axis in the z direction in a model of the insulating transition metal dichalcogenide monolayer materials with a magnetic proximity effect, and show that its width would be enhanced (decreased) when an electric field is applied in the x $(-x)$ direction. We employ the model Hamiltonian $\hat{h} = \hat{h}_0 + J\hat{\boldsymbol{\sigma}} \cdot \boldsymbol{m}$, where $\hat{h}_0$ is a six-band tight-binding Hamiltonian suitable for the low-energy physics in monolayers of AB_2 (A = Mo, W; B = S, Se, Te), as was detailed in Ref. [46]. Considering a right-handed up-down Néel-type wall with easy axis in the z direction, the induced spin is plotted in Fig. 4 under an electric field in the positive x direction. With the lowest two bands filled, the first Chern form contribution vanishes. The dominant component δs_x is antisymmetric on the two sides of the domain wall center. Thus the torque exerted on magnetization $\delta\boldsymbol{\tau} = \delta\boldsymbol{s} \times \boldsymbol{m}$ is in the positive y direction on both sides, increasing the width of the domain wall. Apparently, when the electric field is reversed, the width of the domain wall is decreased.

V. CONCLUSION

In conclusion, we have studied nondissipative electric driving of magnetization motion in uniform and nonuniform magnetic insulators due to nontrivial topologies of occupied Bloch states in the combined space of crystal momentum and magnetization configuration. The resultant nonconservative electrical generalized force is capable of supporting sustained magnetization motion even in the presence of Gilbert damping. A minimal model has been exploited to show explicitly the limit-cycle behavior of magnetic evolution. For magnetic textures, there is an additional nonconservative and nondissipative electrical generalized force, related to a Chern-Simons DMI for non-Chern insulators in the presence of an electric field.

ACKNOWLEDGMENTS

We thank H. Chen, P. Yan, Y. Cao, L. Dong, and T. Chai for useful discussions. This work is supported by NSF (EFMA-1641101) and Welch Foundation (F-1255).

[1] H. Katsura, N. Nagaosa, and A. V. Balatsky, Phys. Rev. Lett. **95**, 057205 (2005).
[2] M. Mostovoy, Phys. Rev. Lett. **96**, 067601 (2006).
[3] Y. Yamasaki, H. Sagayama, T. Goto, M. Matsuura, K. Hirota, T. Arima, and Y. Tokura, Phys. Rev. Lett. **98**, 147204 (2007).
[4] I. Žutić, J. Fabian, and S. Das Sarma, Rev. Mod. Phys. **76**, 323 (2004).
[5] Y. H. Liu, Y. Q. Li, and J. H. Han, Phys. Rev. B **87**, 100402(R) (2013).
[6] A. Manchon and S. Zhang, Phys. Rev. B **78**, 212405 (2008).
[7] I. Garate and A. H. MacDonald, Phys. Rev. B **80**, 134403 (2009).
[8] H. Kurebayashi *et al.*, Nat. Nanotechnol. **9**, 211 (2014).
[9] C. O. Avci, A. Quindeau, C.-F. Pai, M. Mann, L. Caretta, A. S. Tang, M. C. Onbasli, C. A. Ross, and G. S. D. Beach, Nat. Mater. **16**, 309 (2017).
[10] Q. Shao *et al.*, Nat. Commun. **9**, 3612 (2018).
[11] I. Garate and M. Franz, Phys. Rev. Lett. **104**, 146802 (2010).
[12] T. Yokoyama, J. Zang, and N. Nagaosa, Phys. Rev. B **81**, 241410(R) (2010).
[13] Y. Tserkovnyak and D. Loss, Phys. Rev. Lett. **108**, 187201 (2012).
[14] R. Bustos-Marun, G. Refael, and F. von Oppen, Phys. Rev. Lett. **111**, 060802 (2013).
[15] L. Arrachea and F. von Oppen, Phys. E **74**, 596 (2015).
[16] D. J. Thouless, Phys. Rev. B **27**, 6083 (1983).
[17] X.-L. Qi, T. L. Hughes, and S.-C. Zhang, Nat. Phys. **4**, 273 (2008).
[18] Q. Meng, S. Vishveshwara, and T. L. Hughes, Phys. Rev. B **90**, 205403 (2014).
[19] N. Bode, S. V. Kusminskiy, R. Egger, and F. von Oppen, Phys. Rev. Lett. **107**, 036804 (2011).
[20] J.-P. Hanke, F. Freimuth, C. Niu, S. Blugel, and Y. Mokrousov, Nat. Commun. **8**, 1479 (2017).
[21] R. D. King-Smith and D. Vanderbilt, Phys. Rev. B **47**, 1651 (1993).
[22] S. Onoda, S. Murakami, and N. Nagaosa, Phys. Rev. Lett. **93**, 167602 (2004).

[23] D. Xiao, J. Shi, D. P. Clougherty, and Q. Niu, Phys. Rev. Lett. **102**, 087602 (2009).
[24] G. E. Volovik, J. Phys. C **20**, L83 (1987).
[25] R. A. Duine, Phys. Rev. B **77**, 014409 (2008).
[26] Y. Tserkovnyak and M. Mecklenburg, Phys. Rev. B **77**, 134407 (2008).
[27] S. A. Yang, G. S. D. Beach, C. Knutson, D. Xiao, Q. Niu, M. Tsoi, and J. L. Erskine, Phys. Rev. Lett. **102**, 067201 (2009).
[28] I. Dzyaloshinskii, J. Phys. Chem. Solids **4**, 241 (1958).
[29] T. Moriya, Phys. Rev. **120**, 91 (1960).
[30] F. Freimuth, R. Bamler, Y. Mokrousov, and A. Rosch, Phys. Rev. B **88**, 214409 (2013).
[31] F. Freimuth, S. Blugel, and Y. Mokrousov, J. Phys.: Condens. Matter **26**, 104202 (2014).
[32] B. Xiong, H. Chen, X. Li, and Q. Niu, Phys. Rev. B **98**, 035123 (2018).
[33] Q. Niu, X. Wang, L. Kleinman, W.-M. Liu, D. M. C. Nicholson, and G. M. Stocks, Phys. Rev. Lett. **83**, 207 (1999).
[34] G. V. Karnad, F. Freimuth, E. Martinez, R. Lo Conte, G. Gubbiotti, T. Schulz, S. Senz, B. Ocker, Y. Mokrousov, and M. Klaui, Phys. Rev. Lett. **121**, 147203 (2018).
[35] N. Kato, M. Kawaguchi, Y.-C. Lau, T. Kikuchi, Y. Nakatani, and M. Hayashi, Phys. Rev. Lett. **122**, 257205 (2019).
[36] F. Freimuth, S. Blugel, and Y. Mokrousov, Phys. Rev. B **102**, 245411 (2020).
[37] T. Yoda, T. Yokoyama, and S. Murakami, Sci. Rep. **5**, 12024 (2015).
[38] J. Lee, Z. Wang, H. Xie, K. F. Mak, and J. Shan, Nat. Mater. **16**, 887 (2017).
[39] K. Shiratori and E. Kita, J. Phys. Soc. Jpn. **48**, 1443 (1980).
[40] X.-L. Qi, T. L. Hughes, and S.-C. Zhang, Phys. Rev. B **78**, 195424 (2008).
[41] H. B. Braun, Adv. Phys. **61**, 1 (2012).
[42] S. A. Yang, G. S. D. Beach, C. Knutson, D. Xiao, Z. Zhang, M. Tsoi, Q. Niu, A. H. MacDonald, and J. L. Erskine, Phys. Rev. B **82**, 054410 (2010).
[43] Generally, the pumped electric current is found to be of Hall type $\boldsymbol{j} = \boldsymbol{E} \times \boldsymbol{\sigma}^H$ in response to the artificial electric field from the time-dependent magnetic texture $\mathfrak{E}_\beta = \frac{1}{2}\hat{\boldsymbol{m}} \cdot (\partial_\beta \hat{\boldsymbol{m}} \times \partial_t \hat{\boldsymbol{m}})$ (see, e.g., Ref. [26]), with the Hall conductivity given by $\sigma^H_\gamma = \frac{em^2}{2}\epsilon_{\alpha\beta\gamma}\epsilon_{ijl}\int [d\boldsymbol{k}]\Omega_{k_\alpha k_\beta m_i m_j}\hat{m}_l$. Interestingly, the induced local charge density induced in a magnetic texture [30] $\rho = -e\int [d\boldsymbol{k}]\frac{1}{2}\Omega_{k_i k_j r_j r_i}$ is proportional to the artificial magnetic field, $\mathfrak{B}_\gamma = \frac{1}{4}\epsilon_{\alpha\beta\gamma}\hat{\boldsymbol{m}} \cdot (\partial_\alpha \hat{\boldsymbol{m}} \times \partial_\beta \hat{\boldsymbol{m}})$. We notice a Streda formula relating the two phenomena $\frac{\partial \rho}{\partial \mathfrak{B}_\gamma} = \sigma^H_\gamma$.
[44] B.-J. Yang and N. Nagaosa, Phys. Rev. B **84**, 245123 (2011).
[45] Under a gauge transformation of the wave functions, the Berry connections acquire additional terms given by the gradients of a phase field in the combined $\boldsymbol{k}$ and $\boldsymbol{m}$ space. This phase is modulo 2π in the $\boldsymbol{k}$ space because of the periodic gauge, and the $\boldsymbol{k}$ integral of these additional terms reduces to a partial derivative of some scalar field in the $\boldsymbol{m}$ space. Ordinarily, such a derivative term for the DMI coefficient is permissible, because that would result in an immaterial total gradient in the DMI energy density. When singularities occur as discussed in the example of the previous section, this scalar field can be multivalued over multiply connected regular regions, rendering the DMI energy also multivalued.
[46] G. B. Liu, W. Y. Shan, Y. Yao, W. Yao, and D. Xiao, Phys. Rev. B **88**, 085433 (2013).